Original Article

Rho kinase inhibition ameliorates vascular remodeling and blood pressure elevations in a rat model of apatinib-induced hypertension

Caie Li[a], Liping Ma[a,b], Qiongying Wang[a], Xuejiao Shao[a], Lu Guo[a], Jianshu Chen[a], Wenjuan Wang[a], and Jing Yu[a]

Objectives: Hypertension is one of the major adverse effects of tyrosine kinase inhibitors (TKIs) targeting vascular endothelial growth factors. However, the mechanism underlying TKIs-induced hypertension remains unclear. Here, we explored the role of the RhoA/Rho kinase (ROCK) signaling pathway in elevation of blood pressure (BP) induced by apatinib, a selective TKI approved in China for treatment of advanced or metastatic gastric cancer. A nonspecific ROCK inhibitor, Y27632, was then combined with apatinib and its efficacy in alleviating apatinib-induced hypertension was evaluated.

Methods: Normotensive female Wistar–Kyoto rats were exposed to two different doses of apatinib, or apatinib combined with Y27632, or vehicle for 2 weeks. BP was monitored by a tail-cuff plethysmography system. The mRNA levels and protein expression in the RhoA/ROCK pathway were determined, and vascular remodeling assessed.

Results: Administration of either a high or low dose of apatinib was associated with a rapid rise in BP, reaching a plateau after 12 days. Apatinib treatment mediated upregulation of RhoA and ROCK II in the mid-aorta, more significant in the high-dose group. However, ROCK I expression showed no statistically significant differences. Furthermore, the mRNA level of GRAF3 decreased dose-dependently. Apatinib administration was also associated with decreased levels of MLCP, and elevated endothelin-1 (ET-1) and collagen I, which were accompanied with increased mid-aortic media. However, treatment with Y27632 attenuated the above changes.

Conclusion: These findings suggest that activation of the RhoA/ROCK signaling pathway could be the underlying mechanism of apatinib-induced hypertension, while ROCK inhibitor have potential therapeutic value.

Keywords: apatinib, hypertension, RhoA/Rho-associated coiled-coil domain-containing protein kinase signaling pathway, tyrosine kinase inhibitors, vascular endothelial growth factor

Abbreviations: BP, blood pressure; eNOS, endothelial nitric oxide synthase; ET-1, endothelin-1; ETA, endothelin A receptor; GAPsGTP, ase-activating proteins; GDP, guanosine diphosphate; GDI, sguanine dissociation inhibitors; GEF, sguanine nucleotide exchange factors; GTP, guanosine triphosphate; HR, heart rate; MBP, mean blood pressure; MLC, myosin light chain; MLCP, myosin light chain phosphatase; MMP, matrix metalloproteinase; NO, nitric oxide; PVDF, polyvinylidene fluoride; qRT-PCR, quantitative real-time PCR; ROCK, Rho-associated coiled-coil domain-containing protein kinase; TKIs, tyrosine kinase inhibitors; VEGF, vascular endothelial growth factors; VSMC, vascular smooth muscle cell

INTRODUCTION

Vascular endothelial growth factors (VEGF) play a critical rule in tumor growth and metastasis. Although tyrosine kinase inhibitors (TKIs) with anti-VEGF activity have shown excellent antitumor effects in various cancers, they have been associated with several cardiovascular events [1], such as hypertension, with reported incidences as high as 11–45% [2]. Increased blood pressure (BP) not only causes discontinuation of antitumor therapy but also exacerbates occurrence of cardiovascular events. Although some treatment strategies for TKIs-induced hypertension have been recommended, none of them have sufficient evidence [2,3]. Blood pressure is poorly controlled in many patients, increasing the demand for identification of new substances for treatment of TKIs-induced hypertension.

To date, little is known regarding the mechanism underlying TKIs-induced hypertension. Notably, mounting evidences suggest that activation of the renin–angiotensin

system or the sympathetic nervous system has little effect on its pathogenesis, distinguishing it from primary hypertension [4–6]. Inhibition of nitric oxide (NO) pathway, and activation of endothelin pathway, as well as vascular rarefaction, renal function impairment caused by glomerular injury, and increased salt sensitivity, are some of the proposed underlying mechanisms [7]. Among them, inhibition of NO synthesis and activation of endothelin-1 (ET-1) secretion are the most widely studied.

RhoA is a member of the Rho family regulated by guanosine triphosphate (GTP) binding and cycles between the active GTP-bound form and the inactive guanosine diphosphate (GDP)-bound form. This cycle is directly controlled by three groups of regulatory proteins, namely guanine nucleotide exchange factors (GEFs), guanine dissociation inhibitors (GDIs), and GTPase-activating proteins (GAPs). Functionally, GEFs activate RhoA by facilitating exchange of GDP for GTP, GDIs maintain RhoA in an inactive state, whereas GAPs promote RhoA's intrinsic GTPase activity to hydrolyze GTP into GDP [8]. Previous studies have shown that *Arhgap42* (also known as *GRAF3*) is a Rho-specific GAP involved in the occurrence of hypertension [9]. RhoA mainly interacts with two isoforms of Rho-associated coiled-coil domain-containing protein kinases (ROCK I and ROCK II), to induce phosphorylation with myosin light chain phosphatase (MLCP), thus leading to its inhibition. MLCP then dephosphorylates the myosin light chain (MLC), thereby causing relaxation of vascular smooth muscles [10]. Apart from mediating smooth muscle contraction, activation of the RhoA/ROCK signaling pathway also induces other vascular processes, including endothelial nitric oxide synthase (eNOS) inhibition, endothelial dysfunction and vascular remodeling [11].

Recent research evidences have shown that RhoA/ROCK signaling in the vasculature is a potential target for therapeutic intervention of salt-sensitive hypertension [12]. On the other hand, Lankhorst *et al.* [13] demonstrated that sunitinib-induced hypertension has a similar mechanism with salt-sensitive hypertension and could be aggravated by high-salt intake. Therefore, we hypothesized that the RhoA/ROCK signaling pathway could be mediating vascular contraction and remodeling in TKIs-induced hypertensive rats, while ROCK inhibitors could lower BP and inhibit vascular remodeling. We, thus evaluated BP responses at different doses of apatinib, a TKI used for antitumor therapy, in normotensive Wistar–Kyoto rats. Furthermore, we explored whether activation of the RhoA/ROCK signaling pathway is the underlying mechanism of apatinib-induced hypertension. Finally, we combined apatinib with Y27632, a nonspecific ROCK inhibitor, to determine its efficacy in reducing apatinib-induced hypertension.

MATERIALS AND METHODS

Animals
All animal experiments were performed according to the guidelines of the National Institutes of Health (NIH) Guide for the Care and Use of Laboratory Animals, while study procedures were approved by the Animal Ethics Committee of Lanzhou University Second Hospital. A total of 40 female Wistar–Kyoto rats, weighing 200 ± 20 g, were obtained from Lanzhou Veterinary Research Institute of Chinese Academy of Agricultural Sciences. The animals were housed at our animal center under controlled conditions of room temperature (22 °C), relative humidity (60%) and a 12 h light/12 h dark cycle. They were fed on standard laboratory rat chows (Beijing Keao Xieli Feed Co, Ltd, Beijing, China) and tap water provided ad libitum, unless stated otherwise. Only female rats were used as apatinib-induced hypertension is not influenced by sex. The rats were randomly divided into five groups ($n = 8$ in each group) after one day of adaptive feeding. High (30 mg/kg per day diluted in 2 ml of 0.9% saline solution) or low (15 mg/kg per day diluted in 2 ml of 0.9% saline solution) doses of apatinib were administered to the first two groups via oral gavage, whereas Y27632 (10 mg/kg per day) was administered to the following two groups via intraperitoneal injection on top of apatinb. Rats in the last group received 2 ml of 0.9% saline solution per day via oral gavage. All the treatments lasted for 15 days.

Blood pressure monitoring
Each rat's body weight was monitored throughout the study period. Briefly, a tail-cuff plethysmography system (IITC Life Science, Woodland Hills, California, USA) was used to measure SBP, DBP, mean blood pressure (MBP) and heart rate (HR) of conscious rats before (baseline) and throughout the treatment period (after every 3 days). On the 15th day of treatment, the rats were anesthetized with 2% sevoflurane and cannulated from either of the arteria femoralis to monitor MBP invasively. At the end of the experimental period, the animals were sacrificed under an intravenous overdose of pentobarbital, and mid-aorta harvested for further examination.

Determination of *GRAF3*, *RhoA* and *eNOS* mRNA expression
Total RNA was first extracted using the Trizol method, and reverse-transcribed into cDNA using a PrintScriptTM RT Reagent Kit with gDNA Eraser (Takara Bio Inc., Shiga, Japan). The cDNA was subjected to quantitative real-time PCR (qRT-PCR) analysis using the TB Green™ Premix Ex TaqTM II (Takara Bio Inc.), targeting *GRAF3* (*ArhGAP42*), *RhoA* and *eNOS*, with *GAPDH* as the internal amplification control. A list of primers used is shown in Table S1, http://links.lww.com/HJH/B815. All experiments were conducted using the Rotor-Gene-Q PCR platform (Version 2.3.1; Qiagen, Hilden, Germany).

Western blot analysis
Proteins were first extracted from each mid-aorta lysate (20 μg), separated on 10% SDS-PAGE gels, and then transferred to polyvinylidene fluoride (PVDF) microporous membranes (Millipore, Darmstadt, Germany). The membranes were blocked with 5% skim milk, and immunoblotted with the following primary antibodies: RhoA (1:1000, 10749–1-AP, Protein-tech, Wuhan, China), ROCK I (1:1000, ab134181, Abcam, Cambridge, UK), ROCK II (1:20000, ab125025, Abcam), MLCP (1:1000, ab32519, Abcam), endothelin A receptor (ETA, 1:900, ab85163, Abcam), and collagen I (Col I, 1:500, ab6308, Abcam). The membranes were incubated with horseradish

peroxidase (HRP)-conjugated antirabbit or antimouse secondary antibodies (1 : 15000, Protein-tech), and then subjected to chemiluminescence detection using the ECL kit (NcmECL Ultra, NCM Biotech, Suzhou, China). Intensity of immunoreactive bands was normalized using GAPDH expression (1 : 7000, 10494-1-AP, Proteintech), and quantified using densitometry analysis performed with the Image J software (Version 1.53e, NIH, Bethesda, Maryland, USA).

Biochemical measurements

A chemiluminescent ELISA (Elabscience, Wuhan, China) was used to assess plasma ET-1. Briefly, a capture antibody specific to the target protein was attached to a microplate and 100 μl samples, and different concentrations of dilute standards that bind to the capture antibody added to the microplate. Next, the samples were washed to remove unbound substances, followed by the addition of a detection antibody that binds to the immobilized target protein. Excess detection antibody was washed off and HRP substrate added upon HRP conjugation for indirect detection of bound protein. Absorbance was measured at 450 nm, and the concentration of target protein analyzed using the standard signal vs. concentration curve.

Histological analysis of mid-aorta hypertrophy

Mid-aorta tissues were fixed in 10% buffered formalin, embedded in paraffin and cut into 4-μm sections. Resulting sections were stained with one of the following: hematoxylin and eosin (H&E, Solarbio, Beijing, China), Victoria blue elastic fiber dyeing (Solarbio), elastic/collagen double dyeing (Solarbio), or picrosirius red (Leagene Biotechnology, Beijing, China), and then subjected to light microscopy (TissueGnostics, Vienna, Austria) for determination of media thickness and lumen diameter of the aortic lumen. The media thickness/lumen diameter ratio was calculated in each group. Picrosirius red staining was used to determine the collagen content in the aortic media with polarized light microscopy (Carl Zeiss, Jena, Germany).

Statistical analysis

Statistical analyses were performed using SPSS version 25 (IBM, Armonk, New York, USA) and GraphPad Prism version 6.0 (La Jolla, California, USA). Data were presented as means ± standard error of the mean (SEM) or geometric means with 95% confidence intervals (CIs). Differences between two independent groups were determined using an unpaired Student t-test, while one-way or two-way ANOVA followed by either Dunnett or Tukey's post hoc test were used to compare means across multiple groups. Data followed by P less than 0.05 were considered statistically significant.

RESULTS

Effect of apatinib on blood pressure

No mortality occurred during the treatment period. The average rat bodyweight was 201.3 ± 8.7 g at baseline, although this gradually increased with increasing feeding days, reaching 220.6 ± 6.6 g at the end of the intervention. No significant differences were observed in bodyweight across the groups at baseline ($P = 1.0$) and at the end of intervention ($P = 0.97$). Baseline BP was $123.3/69.3 \pm 2.2/3.4$ mmHg in all groups,

while baseline MBP and HR were 86.8 ± 2.0 mmHg and 371.9 ± 11.3 bpm, respectively. Apatinib treatment significantly increased BP from the third to the sixth day, regardless of whether it was SBP, DBP or MBP, reaching a plateau after 12 days. Compared with low-dose apatinib, high-dose apatinib has a more obvious effect on increasing blood pressure. At the end of intervention, the mean MBP was 111.9 ± 3.6 mmHg in high-dose group and 108.1 ± 1.8 mmHg ($P < 0.001$) in low-dose group. The invasive MBP was higher than noninvasive MBP by 23.8 ± 3.3 mmHg, and the trend of differences between groups was consistent with noninvasive measurement (Figure S1, http://links.lww.com/HJH/B814). The increase in BP was accompanied by a significant reduction in HR. Notably, Y27632 significantly abolished the apatinib-induced elevation in BP by 64.6% ($P < 0.001$) in the high-dose group ($\Delta\Delta$MBP, 17.3 ± 3.0 mmHg) and by 69.6% ($P < 0.001$) in the low-dose group ($\Delta\Delta$MBP, 15.5 ± 2.1 mmHg). However, there is still a statistically significant difference in BP between the two groups (95.7 ± 3.9 mmHg vs. 92.9 ± 1.4 mmHg, $P = 0.049$). Although there was no significant statistical difference, the BP in the control group also increased slightly throughout the intervention ($125.0/64.9 \pm 2.0/2.5$ vs. $123.1/65.0 \pm 3.4/3.4$ mmHg, $P = 0.28$). Y27632 did not affect HR in the rats (Fig. 1).

Expression of RhoA/Rho-associated coiled-coil domain-containing protein kinases pathway mRNAs and proteins

The mRNA levels of RhoA and ROCK II in mid-aorta increased at different apatinib doses (both $P < 0.001$ vs. vehicle), more significantly in the high-dose group, while the mRNA level of GRAF3 decreased ($P < 0.001$ vs. vehicle). However, apatinib caused no significant change in mRNA level of ROCK I relative to vehicle (Fig. 2). Similar patterns were observed with regards to expression of RhoA and ROCK II proteins, while ROCK I expression remained the same in all groups (Fig. 3).

Expression of proteins related to vascular contraction and hypertrophy

Apatinib administration downregulated MLCP levels in the mid-aorta while exposure to Y27632 attenuated this effect. Moreover, apatinib upregulated protein levels of ETA but downregulated mRNA levels of eNOS, both were suppressed by Y27632 (Figs. 4 and 5). The concentration of circulating ET-1 was 0.67 ± 0.1 pg/ml at baseline and at the end of treatment in the vehicle group. However, it significantly increased dose-dependently with apatinib administration ($P < 0.01$). Notably, this elevation was attenuated by Y27632 administration (Fig. 6). Furthermore, apatinib significantly upregulated levels of Col I protein, an indicator of vascular hypertrophy, in the mid-aorta but Y27632 treatment attenuated this upregulation (Fig. 4).

Vascular remodeling

The observed patterns of collagen overexpression inspired us to investigate the mechanical metrics of the mid-aorta. Representative historical cross-sections from each group are shown in Fig. 7. Sections stained using H&E (Fig. 7a and b) and Victoria blue (Fig. 7c) both showed intact elastic laminae in all
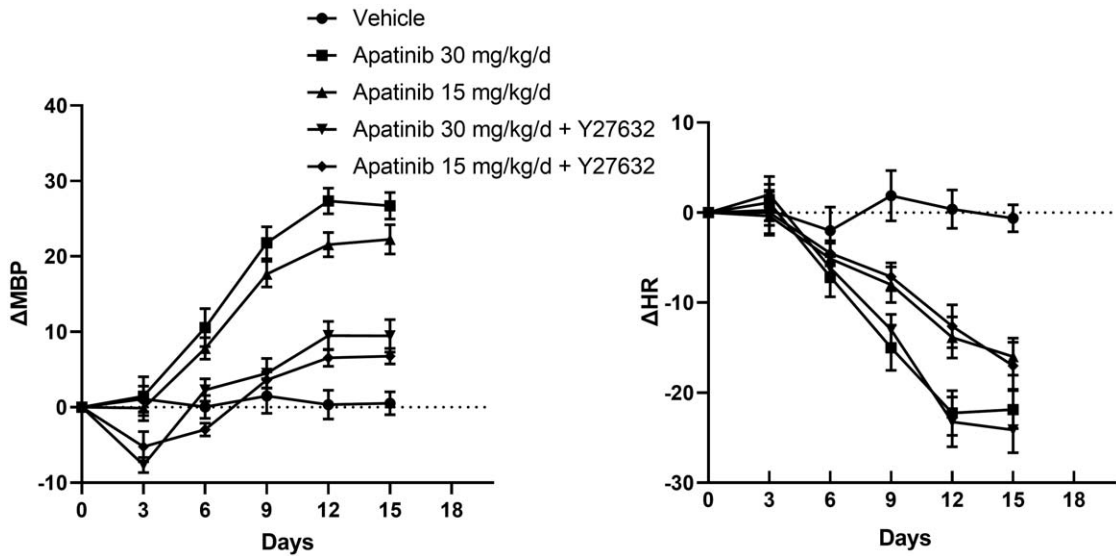
FIGURE 1 Profiles of apatinib-induced changes in mean blood pressure. Apatinib was associated with significant increase in MBP from the third to sixth day of the treatment, reaching a plateau after 12 days. Apatinib also significantly reduced HR. Y27632 mitigated apatinib-induced elevation in BP by 64.6% ($P < 0.001$) in the high-dose group ($\Delta\Delta$MBP, 17.3 ± 3.0 mmHg) and by 69.6% ($P < 0.001$) in the low apatinib group ($\Delta\Delta$MBP, 15.5 ± 2.1 mmHg) but had no effect on the reduced HR ($n = 8$ in each group). HR, heart rate; MBP, mean blood pressure.
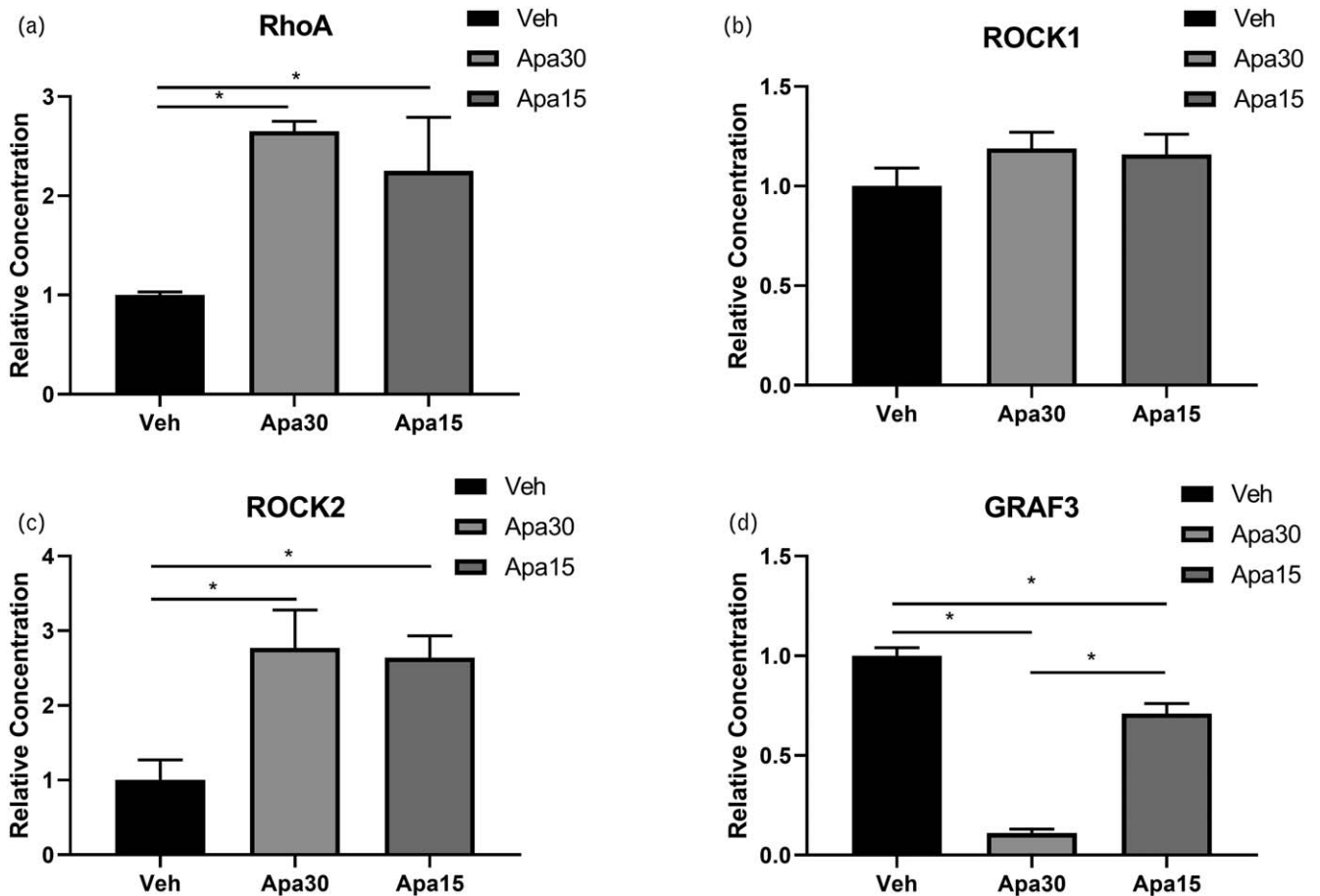

FIGURE 2 Effect of apatinib treatment on level of RhoA and Rho-associated coiled-coil domain-containing protein kinase mRNAs. Apatinib upregulated RhoA and ROCK II mRNAs relative to the vehicle ($P < 0.001$) but downregulated GRAF3 ($P < 0.001$) in the mid-aorta. Apatinib had no effect on level of ROCK I mRNAs between vehicle and treatment groups ($n = 8$ in each group). *P less than 0.05. ROCK, Rho-associated coiled-coil domain-containing protein kinase.
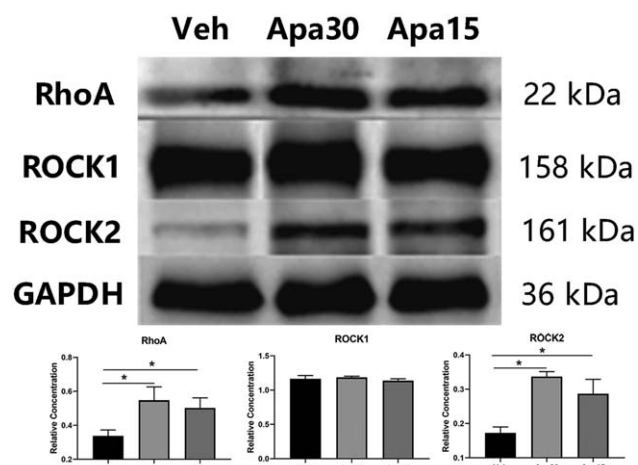
FIGURE 3 Effect of apatinib on expression of proteins in the RhoA/Rho-associated coiled-coil domain-containing protein kinase signaling pathway. Apatinib upregulated expression of RhoA and ROCK II proteins but had no significant effect on ROCK I expression in all groups ($n = 8$ in each group). *P less than 0.05. ROCK, Rho-associated coiled-coil domain-containing protein kinase.
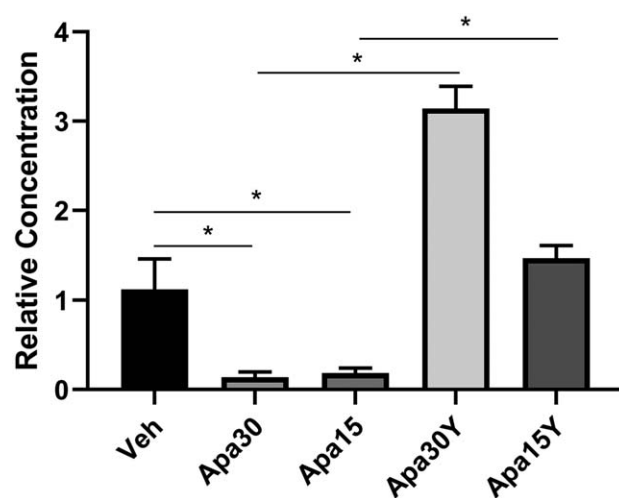

FIGURE 5 Profiles of endothelial nitric oxide synthase mRNA expression. Apatinib treatment downregulated eNOS, while the effect was mitigated by Y27632 ($n = 8$ in each group). *P less than 0.05. eNOS, endothelial nitric oxide synthase.

groups. Notably, 30, but not 15 mg/kg per day of apatinib caused a marked increase in intra-laminae distances. Similarly, only the high dose slightly increased the MT/LD ratio. However, Y27632 reduced the MT/LD ratio in both doses (Fig. 7f). Furthermore, elastic/collagen double dyeing (Fig. 7d) and picrosirius red staining (Fig. 7e) revealed an increase in collagen after high dose treatment, consistent with the increased intralaminar distances. Notably, even the low dose of apatinib treatment increased the percentage of collagen-positive area in the mid-aorta, whereas Y27632 alleviated this alteration in both groups (Fig. 7e and g).

DISCUSSION

Apatinib [AiTan^TM (China); Rivoceranib (global)], a novel, small molecule, and selective TKI targeting VEGF receptor-

2 (VEGFR-2), was the second antiangiogenic drug to be approved in China for treatment of advanced or metastatic gastric cancer [14]. However, the drug is associated with various adverse effects, key among them being hypertension, which reportedly had an incidence of 35.2% in a phase III clinical trial, and is also one of the main reasons for dose reduction [15]. To date, the underlying mechanism of apatinib-induced hypertension remains unclear. Previous studies investigating mechanisms of antiangiogenic agents have mainly focused on another TKI, sunitinib, with upregulation of the ET-1 and downregulation of the NO system getting the most attention [5,16]. In the present study, we sought to evaluate effects of apatinib on BP changes, then explored whether there is another mechanism underlying the change of ET-1 and NO in TKIs-induced hypertension.
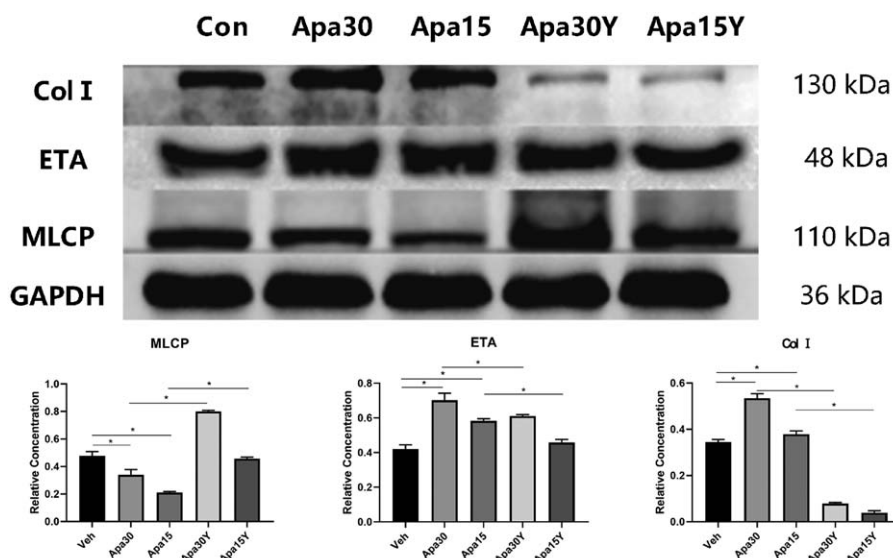

FIGURE 4 Expression of proteins related to vascular contraction and hypertrophy. Western blot showing that apatinib administration mediated downregulation of MLCP in the mid-aorta while Y27632 administration attenuated this tendency. Protein levels of ETA were upregulated with administration of either dose of apatinib and Y27632 mitigated both ($n = 8$ in each group). *P less than 0.05. ETA, endothelin A receptor; MLCP, myosin light chain phosphatase.
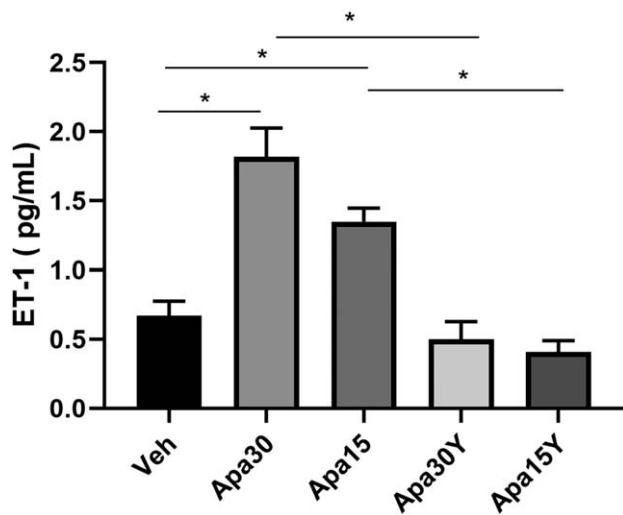
FIGURE 6 Levels of endothelin-1 in plasma. Circulating ET-1 concentration was 0.67 ± 0.1 pg/ml at baseline and the end of treatment in vehicle administration, then significantly increased dose-dependently after apatinib administration ($P < 0.01$). Y27632 attenuated this elevation ($n = 8$ in each group). *P less than 0.05. ET-1, endothelin-1.

Previous antitumor studies have explored apatinib doses of 40–60 mg/kg per day in rats [17,18], 60–100 mg/kg per day in mice [19,20] and 500–750 mg/day (6.7–10 mg/kg per day) in humans [21]. However, a recent study revealed that administration of apatinib, at a dose of 10 or 30 mg/kg per day for 15 days, not only significantly inhibited the growth and proliferation of tumor cells but also promoted their apoptosis in mice [22]. Therefore, we adopted these two doses (30 and 15 mg/kg per day) to explore the effects of apatinib on BP over a 15-day period. In addition, we studied effect of Y27632 on apatinib-induced hypertension, using previously reported doses [9,23,24].

Our results showed that administration of both high (30 mg/kg per day) and low (15 mg/kg per day) doses of apatinib significantly increased BP in rats within 3–6 days, reaching a plateau in 12 days, and this was accompanied by a significant reduction in HR. Compared with low-dose apatinib, high-dose apatinib had a more obvious effect on BP. Y27632 mitigated the apatinib-induced elevation in BP, yet failed to eliminate the differences between the high-dose and low-dose groups. Although without significant statistical differences, BP in the control group also increased slightly throughout the intervention, which may be caused by the intake of saline. Previous studies on sunitinib showed a drug-induced elevation of BP within 2 days of treatment [4,5,7,8,16,25], which was shorter than the present study. This may possibly be because of a relatively higher dose of sunitinib administered in these studies. However, the drug doses in our study were much closer to that of the clinical settings. Despite the time differences in BP rise, our results were consistent with findings from a previous study on sunitinib, which showed that concomitant treatment with the ROCK inhibitor significantly suppressed sunitinib-induced elevation in BP, although it had little effect on sunitinib-induced HR reduction. Therefore, activation of RhoA/ROCK signaling could

be a key mechanism underlying TKIs-induced hypertension [26].

Results from qRT-PCR and western blot analyses revealed that apatinib treatment mediated significant upregulation of RhoA and ROCK II, but there was no change in ROCK I expression. The serine/threonine kinases, ROCK I and ROCK II, are the most widely studied downstream effectors of RhoA. Although they share 60% identity overall, 90% identity within the kinase domain, 100% identity within the ATP binding pocket and share many substrates [8], only ROCK II binds directly to the myosin-binding subunit of MLCP and plays a crucial role in vascular smooth muscle cells (VSMC) contractility [10,27]. Previous studies have shown that activating ROCK II inhibits MLCP activity in a dose-dependent manner, thereby increasing MLC phosphorylation, and increasing contraction [8]. Our results also revealed significant downregulation of MLCP after treatment of both apatinib doses and reversed by concomitant treatment with nonspecific ROCK inhibitor Y27632, confirmed our hypothesis.

GRAF3, a RhoA-specific GAP, specifically expressed in smooth muscle cells, controls BP by limiting RhoA-dependent contractility of resistance arterioles. This suggests that GTPase expression could be acting as a negative feedback mechanism to limit excessive vessel constriction. To this end, a previous study found that *GRAF3*-deficient mice exhibited increased susceptibility to DOCA-salt-mediated hypertension [28]. Results from another in-vivo mouse model showed that even modest induction of *GRAF3* in smooth muscle cells significantly decreased basal BP and vasoconstrictor-induced hypertension, indicating that allosteric activators of *GRAF3* are targeted antihypertensive drugs [29]. Therefore, apatinib could be acting by first activating RhoA via *GRAF3* inhibition thereby causing vascular remodeling, as evidenced by expression of collagen and increased media thickness of mid-aorta. Previous data on vascular remodeling induced by TKIs are quite rare. In a mouse model that simulated tumor by expressing VEGFA with an adenoviral vector, aflibercept, a VEGF Trap, promoted the collapse of angiogenic vessels probably via inhibiting the release of eNOS and affecting endothelial function, accompanied by an elevation of systemic blood pressure [30]. Grisk *et al.* [26] revealed in a rat model that treatment of sunitinib for 4 days can lead to hyalinosis and thickening of the vascular wall of the preglomerular resistance arteries, though the underlying mechanism is unclear. As the development of GRAF3 agonists is more complicated than ROCK antagonists, and the GRAF3 agonists cannot completely prevent RhoA activation, we, therefore, chose ROCK antagonists as the intervention drug.

Apart from RhoA/ROCK pathway, matrix metalloproteinase (MMP) and cathepsins (CatS/CatK) families also play important roles in vascular remodeling. In a mouse model of stress-related vascular aging, the expression of MMP-2/-9 and CatS/CatK in the aorta was significantly increased, which may be related to inflammation and oxidative stress [31]. CatS also participates in the proliferation and migration of VSMC induced by injury through cross-talk with histone deacetylase 6 (HDAC6) [32]. CatK-mediated caspase-8 maturation is a key initial step for oxidative stress-induced smooth muscle cell apoptosis, and is involved in the
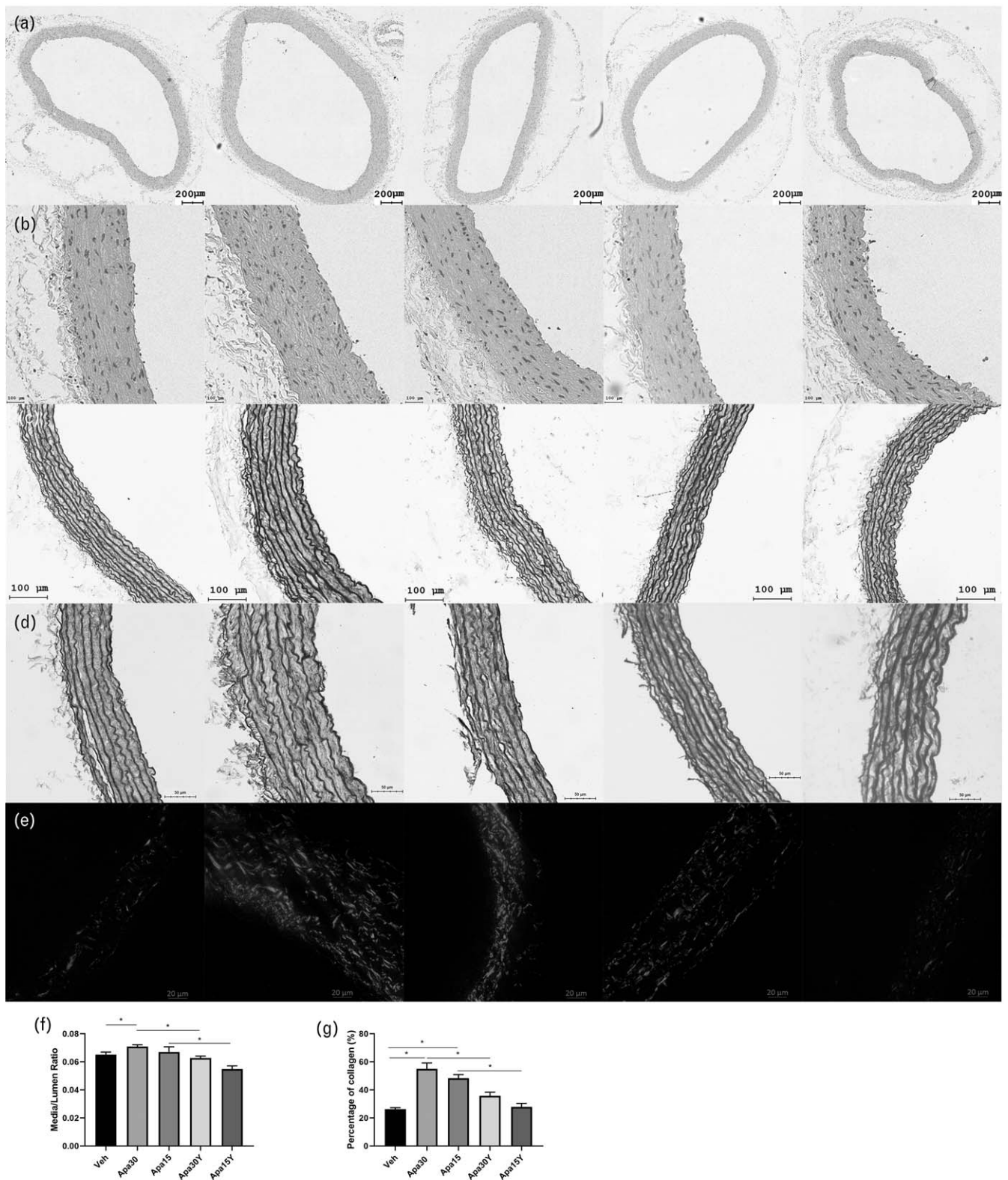
FIGURE 7 Representative histological sections. Sections stained with both H&E (a and b) and Victoria blue (c) revealed intact elastic laminae in all groups. Apatinib at a dose of 30 mg/kg/day caused an increase in intralaminae distances in hypertensive specimens. A high apatinib dose caused a slight increase in the MT/LD ratio but Y27632 administration reduced this ratio in both doses (f). The elastic/collagen double dyeing (d, indicated in red) and picrosirius red staining (e, collagen I in orange-red, and collagen III in green) further revealed increased collagen after high-dose treatment, consistent with the increased intralaminar distances. Percentage of collagen-positive area in the mid-aorta significantly increased even in the low-dose group, while Y27632 alleviated this alteration in both doses (g) ($n = 8$ in each group). MT/LD, media thickness/lumen diameter.

injury-related vascular remodeling and neointimal hyperplasia [33]. CatK even plays an essential role in skeletal muscle repair in response to cardiotoxin injury [34]. Whether MMPs and Cat families are involved in apatinib-related vascular remodeling remains to be further studied.

As a potent vasoconstrictor, ET-1 is mainly produced by vascular endothelial cells, and acts through its two type of receptors, ETA and ETB. When combined with ETA on VSMCs, ET-1 induces vasoconstriction, and when combined with ETB on endothelial cells, it induces NO and prostaglandin production, which leads to vasodilation [35]. Previous studies have demonstrated that increased ET-1 secretion and decreased NO production are the key mechanisms through which TKIs induce hypertension [4,5,16]. Moreover, TKIs with anti-VEGF activities were found to cause endothelial dysfunction, thereby elevating ET-1 and decreasing eNOS, which is essential for NO production, and causing an imbalance between NO and ET-1 [36]. In the present study, apatinib treatment caused a decrease in eNOS but mediated an increase in ETA in the mid-aorta, accompanied by an increase in plasma ET-1 levels.

Furthermore, we explored whether Rho is involved in the changes of NO and ET systems, and found that Y27632 significantly upregulated eNOS expression but downregulated ETA expression in the mid-aorta and ET-1 in plasma, indicating that the RhoA/ROCK signaling pathway could be involved in regulation of the above two. Previous studies have shown that endothelial cells play a crucial role in regulation of vasomotor activity by releasing vasodilator NO and vasoconstrictor ET-1, which is impaired when endothelial dysfunction occurs [37,38]. Additional evidences have also shown that NO production in endothelial cells is a target and effector of RhoA signaling. Notably, activation of RhoA/ROCK was found to downregulate endothelial eNOS expression in endothelial cells by reducing eNOS mRNA stability, while ROCK inhibitors reportedly upregulated eNOS expression [11]. Furthermore, the RhoA/ROCK signaling pathway is involved in the mechanotransduction mechanism involved in the adherence junction strengthening at EC–EC contacts. This endothelial mechanosensing is essential for alignment of EC along the flow direction, thereby promoting vascular homeostasis [39]. Therefore, it is possible that activating the RhoA/ROCK signaling pathway could be related to endothelial dysfunction, which may cause ET-1 upregulation. In addition, there is an interesting link existing between production of NO and secretion of ET-1. Weng *et al.* [40] demonstrated that even very low concentrations of NO could suppress release of ET-1 from human umbilical vein endothelial cells, and this was accompanied by downregulation of preproET-1 mRNA. More experimental results have shown that a decrease in available vascular NO can result in increased ET-1 levels, and the vasoconstriction induced by eNOS blockade with L-arginine analogues is largely because of enhanced ET-1 signaling [41,42]. Overall, these findings indicate that low NO production by endothelial cells could cause increased ET-1 signaling [43]. On the other hand, high level of ET-1 impairs endothelial NO production [44] and ETA siRNA upregulates NO via NOS enzymes [45]. Furthermore, the elevated ET-1 could potentially act as an upstream factor to activate the RhoA/ROCK signaling pathway [46,47], and generate a vicious cycle. Previous results from a transected aorta constriction mouse model showed that activation of the RhoA/ROCK signaling could be playing a central role in enhancing vasoconstriction to ET-1 and impairing endothelial NO-mediated vasodilation. Notably, H-152-mediated ROCK inhibition alleviated the enhanced vasoconstriction to ET-1 and prevented coronary arteriolar constriction to ACh in a manner sensitive to eNOS blocker [48].

Another concern of the ROCK inhibitor is its impact on antitumor therapy. Actually, RhoA/ROCK activation was found to promote metastatic spread and tumor invasion [49], Previous studies have verified activation of the Rho/ROCK signaling pathway in various cancers, including nasopharyngeal carcinoma [50], pancreatic ductal adenocarcinoma [51], neuroblastoma [52], glioblastoma [53] and gastric cancer [54]. Notably, ROCK inhibitors were shown to significantly prevent tumor growth, invasion and metastasis in the aforementioned cancers. Furthermore, ROCK blockade promotes cancer cell phagocytosis and induces antitumor immunity by enhancing T-cell priming via dendritic cells, suppressing tumor growth in syngeneic tumor models [55]. Therefore, ROCK inhibitors may counteract the blood pressure-increasing effects of VEGF antagonists, and promote their antineoplastic effects, indicating that they are the best choice for treatment of TKIs-induced hypertension.

Collectively, results of the present study indicated that apatinib treatment increased BP and promoted vascular remodeling by activating the RhoA/ROCK signaling pathway. However, Y27632, a nonspecific ROCK inhibitor, reversed apatinib-induced increase in BP and vascular remodeling. Therefore, RhoA/ROCK activation could be the underlying mechanism of apatinib-induced hypertension while ROCK inhibitors could be potential therapeutic drugs.

Conflicts of interest
There are no conflicts of interest.

REFERENCES

1. Moslehi JJ. Cardiovascular toxic effects of targeted cancer therapies. *N Engl J Med* 2016; 375:1457–1467.

2. Zamorano JL, Lancellotti P, Rodriguez Munoz D, Aboyans V, Asteggiano R, Galderisi M, *et al.* 2016 ESC Position Paper on cancer treatments and cardiovascular toxicity developed under the auspices of the ESC Committee for Practice Guidelines: the Task Force for cancer treatments and cardiovascular toxicity of the European Society of Cardiology (ESC). *Eur Heart J* 2016; 37:2768–2801.

3. Williams B, Mancia G, Spiering W, Agabiti Rosei E, Azizi M, Burnier M, *et al.* 2018 ESC/ESH Guidelines for the management of arterial hypertension. *Eur Heart J* 2018; 39:3021–3104.

4. Kappers MH, Smedts FM, Horn T, van Esch JH, Sleijfer S, Leijten F, *et al.* The vascular endothelial growth factor receptor inhibitor sunitinib causes a preeclampsia-like syndrome with activation of the endothelin system. *Hypertension* 2011; 58:295–302.

5. Lankhorst S, Kappers MH, van Esch JH, Smedts FM, Sleijfer S, Mathijssen RH, *et al.* Treatment of hypertension and renal injury induced by the angiogenesis inhibitor sunitinib: preclinical study. *Hypertension* 2014; 64:1282–1289.

6. Storkebaum E, Ruiz de Almodovar C, Meens M, Zacchigna S, Mazzone M, Vanhoutte G, *et al.* Impaired autonomic regulation of resistance arteries in mice with low vascular endothelial growth factor or upon vascular endothelial growth factor trap delivery. *Circulation* 2010; 122:273–281.

7. Lankhorst S, Saleh L, Danser AJ, van den Meiracker AH. Etiology of angiogenesis inhibition-related hypertension. *Curr Opin Pharmacol* 2015; 21:7–13.

8. Dee RA, Mangum KD, Bai X, Mack CP, Taylor JM. Druggable targets in the Rho pathway and their promise for therapeutic control of blood pressure. *Pharmacol Ther* 2019; 193:121–134.

9. Bai X, Lenhart KC, Bird KE, Suen AA, Rojas M, Kakoki M, *et al.* The smooth muscle-selective RhoGAP GRAF3 is a critical regulator of vascular tone and hypertension. *Nat Commun* 2013; 4:2910.

10. Wang Y, Zheng XR, Riddick N, Bryden M, Baur W, Zhang X, Surks HK. ROCK isoform regulation of myosin phosphatase and contractility in vascular smooth muscle cells. *Circ Res* 2009; 104:531–540.

11. Loirand G, Pacaud P. The role of Rho protein signaling in hypertension. *Nat Rev Cardiol* 2010; 7:637–647.

12. Johnson AC, Wu W, Attipoe EM, Sasser JM, Taylor EB, Showmaker KC, *et al.* Loss of Arhgef11 in the Dahl salt-sensitive rat protects against hypertension-induced renal injury. *Hypertension* 2020; 75:1012–1024.

13. Lankhorst S, Severs D, Marko L, Rakova N, Titze J, Muller DN, *et al.* Salt sensitivity of angiogenesis inhibition-induced blood pressure rise: role of interstitial sodium accumulation? *Hypertension* 2017; 69:919–926.

14. Scott LJ. Apatinib: a review in advanced gastric cancer and other advanced cancers. *Drugs* 2018; 78:747–758.

15. Li J, Qin S, Xu J, Xiong J, Wu C, Bai Y, *et al.* Randomized, double-blind, placebo-controlled phase iii trial of apatinib in patients with chemotherapy-refractory advanced or metastatic adenocarcinoma of the stomach or gastroesophageal junction. *J Clin Oncol* 2016; 34:1448–1454.

16. Kappers MH, van Esch JH, Sluiter W, Sleijfer S, Danser AH, van den Meiracker AH. Hypertension induced by the tyrosine kinase inhibitor sunitinib is associated with increased circulating endothelin-1 levels. *Hypertension* 2010; 56:675–681.

17. Zhou Y, Wang S, Ding T, Chen M, Wang L, Wu M, *et al.* Evaluation of the effect of apatinib (YN968D1) on cytochrome P450 enzymes with cocktail probe drugs in rats by UPLC-MS/MS. *J Chromatogr B Analyt Technol Biomed Life Sci* 2014; 973C:68–75.

18. Bao SS, Wen J, Lin QM, Li YH, Huang YG, Zhou HY, Hu GX. Evaluation of the effects of apatinib on the pharmacokinetics of venlafaxine and o-desmethylvenlafaxine in SD male rats by UPLC-MS/MS. *Basic Clin Pharmacol Toxicol* 2018; 123:721–726.

19. Zhao S, Ren S, Jiang T, Zhu B, Li X, Zhao C, *et al.* Low-dose apatinib optimizes tumor microenvironment and potentiates antitumor effect of PD-1/PD-L1 blockade in lung cancer. *Cancer Immunol Res* 2019; 7:630–643.

20. Wang Q, Gao J, Di W, Wu X. Antiangiogenesis therapy overcomes the innate resistance to PD-1/PD-L1 blockade in VEGFA-overexpressed mouse tumor models. *Cancer Immunol Immunother* 2020; 69:1781–1799.

21. Hu X, Zhang J, Xu B, Jiang Z, Ragaz J, Tong Z, *et al.* Multicenter phase II study of apatinib, a novel VEGFR inhibitor in heavily pretreated patients with metastatic triple-negative breast cancer. *Int J Cancer* 2014; 135:1961–1969.

22. Cai X, Wei B, Li L, Chen X, Yang J, Li X, *et al.* Therapeutic potential of apatinib against colorectal cancer by inhibiting VEGFR2-mediated angiogenesis and beta-catenin signaling. *Onco Targets Ther* 2020; 13:11031–11044.

23. Nguyen H, Chiasson VL, Chatterjee P, Kopriva SE, Young KJ, Mitchell BM. Interleukin-17 causes Rho-kinase-mediated endothelial dysfunction and hypertension. *Cardiovasc Res* 2013; 97:696–704.

24. Ni M, Zhang J, Huang L, Liu G, Li Q. A Rho-kinase inhibitor reverses learning and memory deficits in a Rat model of chronic cerebral ischemia by altering Bcl-2/Bax-NMDAR signaling in the cerebral cortex. *J Pharmacol Sci* 2018; 138:107–115.

25. Witte J, Muhlbauer M, Braun D, Steinbach A, Golchert J, Rettig R, Grisk O. Renal soluble guanylate cyclase is downregulated in sunitinib-induced hypertension. *J Am Heart Assoc* 2018; 7:e009557.

26. Grisk O, Koenen A, Meissner T, Donner A, Braun D, Steinbach A, *et al.* Rho kinase inhibition mitigates sunitinib-induced rise in arterial pressure and renal vascular resistance but not increased renal sodium reabsorption. *J Hypertens* 2014; 32:2199–2210.

27. Shimizu T, Fukumoto Y, Tanaka S, Satoh K, Ikeda S, Shimokawa H. Crucial role of ROCK2 in vascular smooth muscle cells for hypoxia-induced pulmonary hypertension in mice. *Arterioscler Thromb Vasc Biol* 2013; 33:2780–2791.

28. Bai X, Mangum KD, Dee RA, Stouffer GA, Lee CR, Oni-Orisan A, *et al.* Blood pressure-associated polymorphism controls ARHGAP42 expression via serum response factor DNA binding. *J Clin Invest* 2017; 127:670–680.

29. Dee RA, Bai X, Mack CP, Taylor JM. Molecular regulation of the RhoGAP GRAF3 and its capacity to limit blood pressure in vivo. *Cells* 2020; 9:1042.

30. Sitohy B, Chang S, Sciuto TE, Masse E, Shen M, Kang PM, *et al.* Early actions of anti-vascular endothelial growth factor/vascular endothelial growth factor receptor drugs on angiogenic blood vessels. *Am J Pathol* 2017; 187:2337–2347.

31. Lei Y, Yang G, Hu L, Piao L, Inoue A, Jiang H, *et al.,* FAHA. Increased dipeptidyl peptidase-4 accelerates diet-related vascular aging and atherosclerosis in ApoE-deficient mice under chronic stress. *Int J Cardiol* 2017; 243:413–420.

32. Wu H, Cheng XW, Hu L, Takeshita K, Hu C, Du Q, *et al.* Cathepsin S activity controls injury-related vascular repair in mice via the TLR2-mediated p38MAPK and PI3K-Akt/p-HDAC6 signaling pathway. *Arterioscler Thromb Vasc Biol* 2016; 36:1549–1557.

33. Hu L, Huang Z, Ishii H, Wu H, Suzuki S, Inoue A, *et al.* PLF-1 (Proliferin-1) modulates smooth muscle cell proliferation and development of experimental intimal hyperplasia. *J Am Heart Assoc* 2019; 8:e005886.

34. Ogasawara S, Cheng XW, Inoue A, Hu L, Piao L, Yu C, *et al.* Cathepsin K activity controls cardiotoxin-induced skeletal muscle repair in mice. *J Cachexia Sarcopenia Muscle* 2018; 9:160–175.

35. Davenport AP, Hyndman KA, Dhaun N, Southan C, Kohan DE, Pollock JS, *et al.* Endothelin. *Pharmacol Rev* 2016; 68:357–418.

36. Leon-Mateos L, Mosquera J, Anton Aparicio L. Treatment of sunitinib-induced hypertension in solid tumor by nitric oxide donors. *Redox Biol* 2015; 6:421–425.

37. Yanagisawa M, Kurihara H, Kimura S, Tomobe Y, Kobayashi M, Mitsui Y, *et al.* A novel potent vasoconstrictor peptide produced by vascular endothelial cells. *Nature* 1988; 332:411–415.

38. Giles TD. Aspects of nitric oxide in health and disease: a focus on hypertension and cardiovascular disease. *J Clin Hypertens (Greenwich)* 2006; 8 (12 Suppl 4):2–16.

39. Shimokawa H, Sunamura S, Satoh K. RhoA/Rho-kinase in the cardiovascular system. *Circ Res* 2016; 118:352–366.

40. Weng YH, Kuo CY, Chiu YW, Kuo ML, Liao SL. Alteration of nitric oxide gas on gene expression of endothelin-1 and endothelial nitric oxide synthase by a time- and dose-dependent manner in human endothelial cells. *Chin J Physiol* 2009; 52:59–64.

41. Richard V, Hogie M, Clozel M, Loffler BM, Thuillez C. In vivo evidence of an endothelin-induced vasopressor tone after inhibition of nitric oxide synthesis in rats. *Circulation* 1995; 91:771–775.

42. Cardillo C, Kilcoyne CM, Cannon RO 3rd, Panza JA. Interactions between nitric oxide and endothelin in the regulation of vascular tone of human resistance vessels in vivo. *Hypertension* 2000; 35:1237–1241.

43. Lankhorst S, Kappers MH, van Esch JH, Danser AH, van den Meiracker AH. Mechanism of hypertension and proteinuria during angiogenesis inhibition: evolving role of endothelin-1. *J Hypertens* 2013; 31:444–454.

44. Ramzy D, Rao V, Tumiati LC, Xu N, Sheshgiri R, Miriuka S, *et al.* Elevated endothelin-1 levels impair nitric oxide homeostasis through a PKC-dependent pathway. *Circulation* 2006; 114 (1 Suppl):I319–I326.

45. Li L, Wang X, Zheng L, Li J, Xu M, Rong R, *et al.* Downregulation of endothelin A receptor (ETaR) ameliorates renal ischemia reperfusion injury by increasing nitric oxide production. *Life Sci* 2019; 228:295–304.

46. Wicinski M, Szadujkis-Szadurska K, Weclewicz MM, Malinowski B, Matusiak G, Walczak M, *et al.* The role of Rho-kinase and calcium ions in constriction triggered by ET-1. *Microvasc Res* 2018; 119:84–90.

47. Chen YL, Ren Y, Xu W, Rosa RH Jr, Kuo L, Hein TW. Constriction of retinal venules to endothelin-1: obligatory roles of ETA receptors, extracellular calcium entry, and Rho Kinase. *Invest Ophthalmol Vis Sci* 2018; 59:5167–5175.

48. Tsai SH, Lu G, Xu X, Ren Y, Hein TW, Kuo L. Enhanced endothelin-1/Rho-kinase signalling and coronary microvascular dysfunction in hypertensive myocardial hypertrophy. *Cardiovasc Res* 2017; 113:1329–1337.

49. Campbell H, Fleming N, Roth I, Mehta S, Wiles A, Williams G, *et al.* 133p53 isoform promotes tumour invasion and metastasis via interleukin-6 activation of JAK-STAT and RhoA-ROCK signalling. *Nat Commun* 2018; 9:254.

50. Yuan J, Chen L, Xiao J, Qi XK, Zhang J, Li X, *et al.* SHROOM2 inhibits tumor metastasis through RhoA-ROCK pathway-dependent and -independent mechanisms in nasopharyngeal carcinoma. *Cell Death Dis* 2019; 10:58.

51. Rath N, Munro J, Cutiongco MF, Jagiello A, Gadegaard N, McGarry L, *et al.* Rho kinase inhibition by AT13148 blocks pancreatic ductal adenocarcinoma invasion and tumor growth. *Cancer Res* 2018; 78:3321–3336.

52. Dyberg C, Fransson S, Andonova T, Sveinbjornsson B, Lannerholm-Palm J, Olsen TK, *et al.* Rho-associated kinase is a therapeutic target in neuroblastoma. *Proc Natl Acad Sci U S A* 2017; 114:E6603–E6612.

53. Yu G, Wang Z, Zeng S, Liu S, Zhu C, Xu R, Liu RE. Paeoniflorin inhibits hepatocyte growth factor- (HGF-) induced migration and invasion and actin rearrangement via suppression of c-Met-mediated RhoA/ROCK signaling in glioblastoma. *Biomed Res Int* 2019; 2019:9053295.

54. Hinsenkamp I, Schulz S, Roscher M, Suhr AM, Meyer B, Munteanu B, *et al.* Inhibition of Rho-associated Kinase 1/2 attenuates tumor growth in murine gastric cancer. *Neoplasia* 2016; 18:500–511.

55. Nam GH, Lee EJ, Kim YK, Hong Y, Choi Y, Ryu MJ, *et al.* Combined Rho-kinase inhibition and immunogenic cell death triggers and propagates immunity against cancer. *Nat Commun* 2018; 9:2165.